HOKKAIDO UNIVERSITY

Title	Breakup of land-fast sea ice in Lutzow-Holm Bay, East Antarctica, and its teleconnection to tropical Pacific sea surface temperatures
Author(s)	Aoki, S.
Citation	Geophysical research letters, 44(7), 3219-3227 https://doi.org/10.1002/2017GL072835
Issue Date	2017-04-07
Doc URL	http://hdl.handle.net/2115/67293
Rights	An edited version of this paper was published by AGU. Copyright (2017) American Geophysical Union. Aoki, S. (2017), Breakup of land-fast sea ice in Lützow-Holm Bay, East Antarctica, and its teleconnection to tropical Pacific sea surface temperatures, Geophys. Res. Lett., 44, 3219–3227. To view the published open abstract, go to http://dx.doi.org and enter the DOI. DOI:10.1002/2017GL072835.10.1002/2017GL072835.
Type	article
File Information	Aoki-2017-Geophysical_Research_Letters.pdf

Instructions for use

Hokkaido University Collection of Scholarly and Academic Papers : HUSCAP

AGU PUBLICATIONS

Geophysical Research Letters

RESEARCH LETTER
10.1002/2017GL072835

Key Points:
- Poleward extent of land-fast sea ice breakup in Lützow-Holm Bay was strongly correlated with tropical sea surface temperature
- Comparing reconstructed breakup latitudes with tropical ocean temperature explained calving of an inflowing glacier tongue
- Multidecadal changes in calving front location were consistent with those in tropical ocean temperature

Correspondence to:
S. Aoki,
shigeru@lowtem.hokudai.ac.jp

Citation:
Aoki, S. (2017), Breakup of land-fast sea ice in Lützow-Holm Bay, East Antarctica, and its teleconnection to tropical Pacific sea surface temperatures, *Geophys. Res. Lett.*, *44*, 3219–3227, doi:10.1002/2017GL072835.

Received 26 JAN 2017
Accepted 17 MAR 2017
Accepted article online 21 MAR 2017
Published online 7 APR 2017

©2017. American Geophysical Union. All Rights Reserved.

Breakup of land-fast sea ice in Lützow-Holm Bay, East Antarctica, and its teleconnection to tropical Pacific sea surface temperatures

S. Aoki[1]

[1]Institute of Low Temperature Science, Graduate School of Environmental Science, Hokkaido University, Sapporo, Japan

Abstract A large land-fast sea ice breakup occurred in 2016 in Lützow-Holm Bay, East Antarctica. The breakup caused calving from the Shirase Glacier Tongue. Although similar breakups and calving have been observed in the past, the timing and magnitudes are not well-constrained. The ice's breakup latitude during 1997–2016 was analyzed to investigate the variables controlling breakup and examine correlation with local calving for a longer period. The breakup latitude in April had a persistently high correlation with sea surface temperature (SST) in the tropical Pacific, which exceeds correlations with local atmospheric variables. The years of five out of six observed calving events from the mid-20th century can correspond to those of warm SST episodes and calving-front retreat in the 1980s to warmer SST shift. Our proposed teleconnection between tropical SST and Antarctic sea ice could lead to better predictions of breakup and might impact the glacier flux for a wider region.

Plain Language Summary Land-fast sea ice forms along the Antarctic coast, and it occasionally breaks up significantly. The breakup event influences the flow of glaciers, which is otherwise held back by the fast ice. The breakup of land-fast sea ice and the discharge of glaciers have significant multidecadal variability as well as interannual variability. This study explores what controls the breakup phenomena of land-fast sea ice in Antarctica and finds the linkage with tropical sea surface temperatures. We find the environmental factors which are relevant to the ice breakup, and those variables are originally driven by the teleconnection from the tropical Pacific. We believe that our study makes a significant contribution in climate science by offering a causal mechanism that explains the previously observed multidecadal variability in ice extent in this region. Our model can explain five out of the last six calving events in a major glacier connected to this bay, offering hope for future predictions of ice behavior. This will also merit the logistics to Antarctic research stations.

1. Introduction

Land-fast sea ice forms along the Antarctic coast, where it is attached to the land or ice front; it also forms between ice structures including glaciers, ice tongues, and grounded icebergs. Around Antarctica, this ice reaches its maximum area (near 550,000 km^2) in November [*Fedotov et al.*, 1998], representing around 3% of the maximum pack ice area. The spatial patterns and timing of such ice formation and breakup are influenced by atmospheric and oceanic forcing [e.g., *Massom et al.*, 2009; *Fraser et al.*, 2012].

Recently, from March to April 2016, a large portion of land-fast sea ice broke up in Lützow-Holm Bay off Queen Maud Land, East Antarctica (Figure 1), after several years of relative stability. A breakup of comparable magnitude last occurred in 1998 [*Enomoto et al.*, 2002]. The land-fast sea ice edge usually tends to form along the isobaths of the continental shelf's edge, but the passage of low pressure systems often causes ice breakup. The stability of this ice also relates to a quasiperiodicity with alternating stable and unstable periods [*Ushio*, 2006]: the unstable period here was defined as the time when land-fast ice breakup extends poleward beyond 68°50′S. Long-term variations in atmospheric forcing such as air temperature, frequency of southerly winds, and changes in sea ice thickness/structure can be responsible for this quasiperiodicity. For some breakup events, the effects of swell [*Higashi et al.*, 1982] and surface snow melting [*Enomoto et al.*, 2002] have also been discussed. However, there is insufficient quantitative estimation for the multidecadal variability of breakup magnitude and the timing of these events remains unpredictable.

Interannual variations within the Antarctic atmosphere and ocean are strongly influenced by the El Niño–Southern Oscillation (ENSO) and the Southern Hemisphere Annular Mode (SAM, also known as the

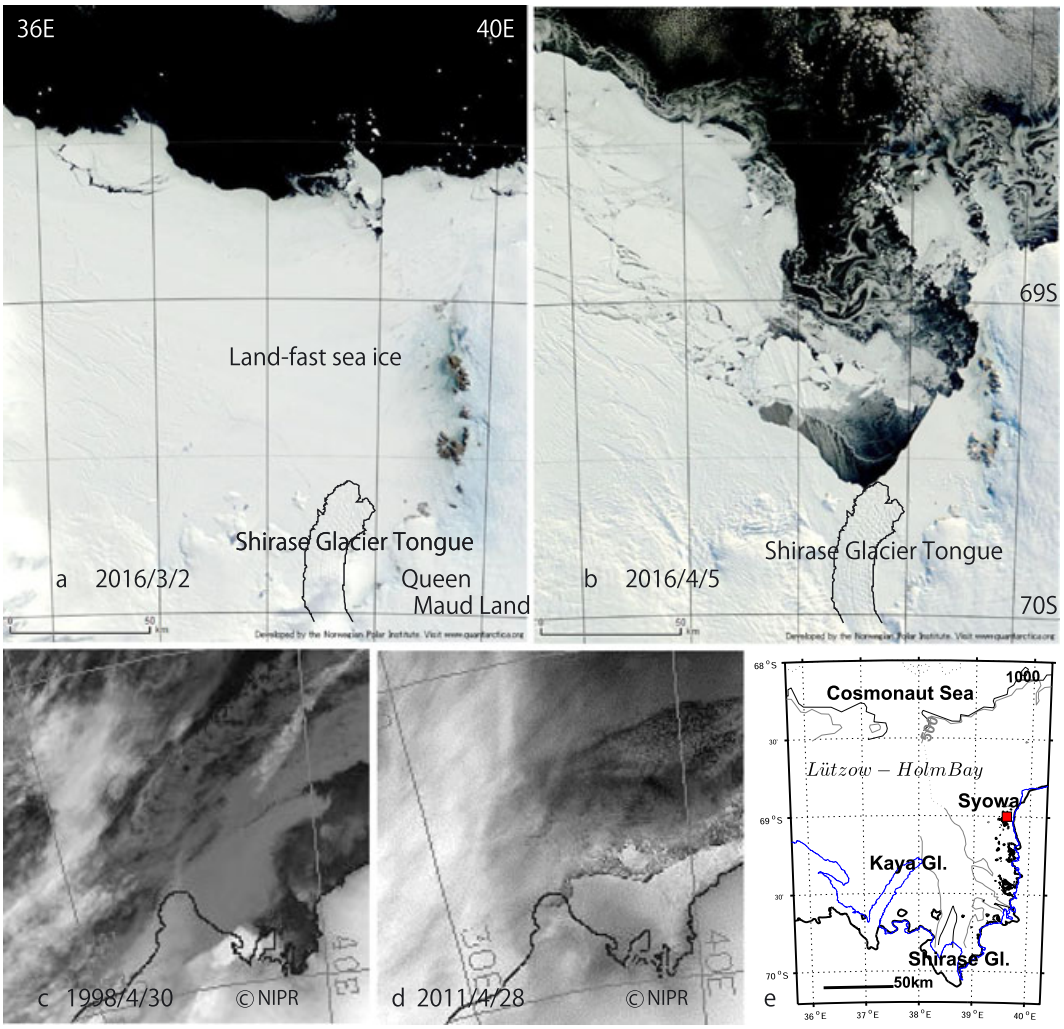

Figure 1. Land-fast sea ice conditions and surroundings in Lützow-Holm Bay off Queen Maud Land, East Antarctica. (a) Aqua MODIS image before the recent breakup on 2 March 2016 and (b) after the breakup on 5 April 2016. NOAA AVHRR images of (c) a large ice breakup case on 30 April 1998 and (d) an insignificant breakup on 28 April 2011. (e) Underlying bathymetry (referring to *Moriwaki and Yoshida* [1990]) with Syowa Station (marked with square).

Antarctic Oscillation, AAO) [e.g., *Turner*, 2004; *Bajish et al.*, 2013; *Welhouse et al.*, 2016]. These climate modes influence changes within Antarctic land-fast sea ice: along the coast of Adélie Land, ice extent was strongly correlated with the SAM index (0.76) averaged over a June–December period for 8 years from 1992 to 1999 [*Massom et al.*, 2009]. In the Indian Ocean sector, there is a correlation (0.45) between such ice extent and the Southern Oscillation Index (SOI) for 9 years from 2000 to 2008 [*Fraser*, 2011]. Therefore, these climate modes are highly likely to affect the land-fast sea ice conditions in Lützow-Holm Bay, and hence, longer period studies are needed to examine the relationship with climatological forcing and to ensure statistical robustness of any conclusions.

The breakup of land-fast sea ice affects the discharge of ice shelves and glaciers to the open ocean. For example, in Porpoise Bay off Wilkes Land, ice breakup was observed before a large calving event of outlet glaciers [*Miles et al.*, 2016]. A similar pattern occurred in Lützow-Holm Bay, which is the terminus for Shirase Glacier, one of the fastest flowing (2.5 km yr^{-1}) outlet glaciers in Antarctica [*Nakawo et al.*, 1978] with freshwater export of 12 Gt/yr [*Nakamura et al.*, 2016]. Calving discharge to the ocean correlates to land-fast sea ice breakup: since the bathymetry in the bay deepens toward the grounding line of the Shirase Glacier, the expansion of ice breakup inevitably proceeds toward the grounding line and thus influences the calving front of the Shirase Glacier Tongue (SGT). During the 2016 breakup, only a small portion calved from the SGT due to

a relatively poleward ice front, but a large iceberg (D25) calved off from the neighboring Kaya Glacier. During the 1998 breakup, the SGT was almost entirely calved from its grounding line [*Enomoto et al.*, 2002]. The position of the SGT calving front reveals a significant multidecadal variability influenced by the history of ice breakup [*Ushio et al.*, 2006], but the causes of this periodicity have not been explained.

The breakup of land-fast sea ice in Lützow-Holm Bay was quantified by using continuous satellite imagery from the late 1990s onward and compared the breakup record with climatological conditions and indices of climate modes. I also attempted to reconstruct the breakup configuration by using regression analysis and assessed it by using location data for the SGT calving front since the 1950s to examine whether environmental forcing can explain the multidecadal variability noted above. The occurrence or absence of ice breakup defines the subsequent growth of sea ice, which directly affects the logistics of Japan's Syowa Station north of the glacier's mouth (69°00′S, 39°35′E); hence, the estimation and prediction of land-fast sea ice breakup in Lützow-Holm Bay are critical.

2. Data and Methods

2.1. Land-Fast Sea Ice Breakup and Its Index

Satellite imagery was used to examine the development of land-fast sea ice breakup in Lützow-Holm Bay for a roughly 20 year period from March 1997 to September 2016. The breakup process varies depending on season and year. From summer to autumn the ice usually breaks up poleward, with the broken ice floes drifting away, and so the process develops almost sequentially, with some exceptions. From winter to spring, in contrast, the ice does break at times, but the broken floes do not drift away and eventually join the solid ice again.

In this study I focused on the open water area (including leads/cracks) which has pack-ice area equatorward or penetrates poleward into the land-fast sea ice, as seen in NOAA advanced very high resolution radiometer (AVHRR) images (Figure 1). Then the southernmost open water intrusion between 36°E and 39°50′E was defined as the breakup point and the position was read by eye by using graphical software. This latitude (defined hereafter as breakup latitude) was used in the analysis since it clearly represents the breakup extent and is directly connected to the advance and retreat of the SGT. The longitude of the breakup point and ice area were not discussed here.

Although relevant imagery has been obtained intermittently since 1980, no continuous record is available before February 1997, so the time series starts in March of that year. During this subsequent 20 year period, data gaps of more than 3 months existed for July–December 2008, January–May 2014, and January–June 2015. The AVHRR imagery resolution is about 3.4 km; to validate these image readings and interpolate the data gaps, higher resolution Aqua Moderate Resolution Imaging Spectroradiometer (MODIS) images (250 m) from August 2012 to September 2016 were analyzed, although images from May to July in each year were not available.

A monthly time series of the southernmost breakup latitude was constructed by using 1196 AVHRR images and 32 MODIS images with minimal cloud influence. There were 9 months ($<$4%) with no data; when data were not available for a certain month, I substituted the breakup latitude of the previous month. Note that the data series for March were least consistent (not available in 2002, 2003, and 2006), but there was no data gap in April. In addition, 16 AVHRR images taken from 1987–1990 [*Yamanouchi and Seko*, 1992] were also helpful in interpreting the results.

2.2. Atmospheric and Oceanic Forcing

Atmospheric data at Syowa Station were examined by using monthly averages of air temperature, sea surface pressure, and wind speed. Monthly statistics of daily maximum wind speed and its direction were also calculated. Oceanic forcing was studied by using monthly average sea surface temperature (SST) data. I used Optimum Interpolation Sea Surface Temperature Version 2 (OISSTv2, 1982–2016) data for direct comparison with our own observed breakup latitude. To extend the study period before the satellite era, I also consulted the Extended Reconstructed (ERSSTv4, 1854–2016) and Hadley Centre (HadSST3, 1850–2016) SST data sets. Correlations with climate mode indices, including those for ENSO (NINO3, NINO3.4, and NINO4) and SAM (AAO by NOAA Climate Prediction Center), were investigated. Sea ice concentration (SIC) data during 1997–2015 were examined to further ensure the relationship among oceanic variables, using monthly

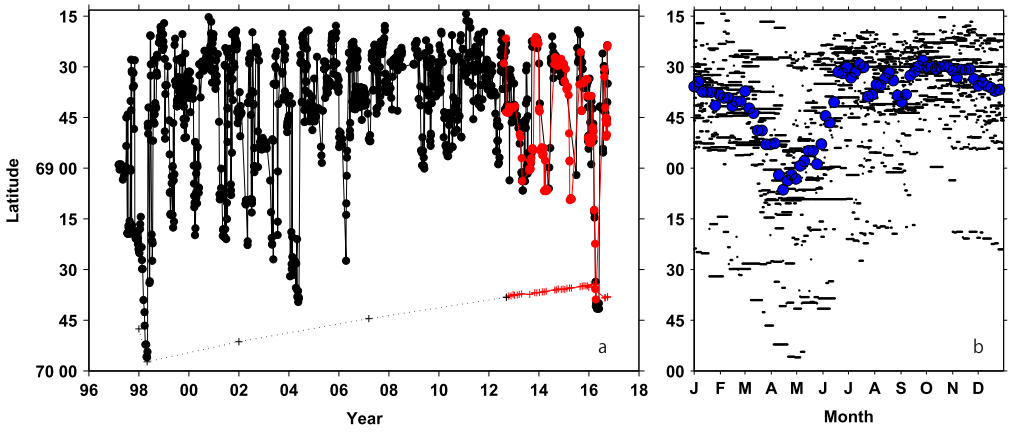

Figure 2. (a) Time series showing the changing latitude of the land-fast sea ice edge (breakup latitude) in Lützow-Holm Bay, sourced from NOAA AVHRR imagery (black dots) and Aqua MODIS imagery (red dots). The crosses show the northernmost calving front of the Shirase Glacier Tongue, sourced from MODIS (red) and other satellite images (black). (b) Seasonal variation of the breakup latitude (black) and its 5 day mean over the whole period (blue).

bootstrap data from Nimbus-7 scanning multichannel microwave radiometer and Defense Meteorological Satellite Program Special Sensor Microwave Imager-Special Sensor Microwave Imager/Sounder.

2.3. Calving Front of Shirase Glacier Tongue

The northernmost latitude of the SGT calving front was examined to assess the potential impact of land-fast sea ice breakup. From 2012 to 2016, this was obtained from the MODIS images, while from 1956 to 1998, this was obtained from *Ushio et al.* [2006, Figure 2]. I supplemented the record with aerial photographs in January 1969, November 1975, and April 1983.

3. Results and Discussion

3.1. Temporal Variations in Land-Fast Sea Ice Breakup

The breakup points in Lützow-Holm Bay were distributed around a longitudinal median of about 38°10′E. This range narrowed poleward, converging to the grounding line of the Shirase Glacier. Breakup latitude (positive southward) exhibited significant seasonal variation (Figure 2). It starts to shift southward in December, accelerates in March, and reaches its maximum in April; from July to October the breakup latitude is relatively stable in the northerly position. This seasonal cycle is consistent with that of land-fast ice area along the East Antarctic coast [*Fraser et al.*, 2012].

The interannual variation of monthly breakup latitude was largest in April, reaching its most southerly position in 1998, 2004, and 2016 (Figure 3a). The pattern of breakup latitude revealed a multidecadal variation: it stayed in a relatively southerly position from 1997 to 2004, before advancing to a more northerly position from 2007 to 2012, and gradually returning south through 2016. Effective sampling size of the time series of April breakup latitude, by a conventional method [e.g., *Trenberth*, 1984], was estimated to be no less than the original data length, although it is difficult to estimate reliably [*Thiebaux and Zwiers*, 1984]. The April breakup latitude was also correlated with that of the preceding summer. The lag correlation coefficient was 0.82 ($n = 20$) with the March breakup latitude and 0.50 ($n = 19$) with December latitude, although it decreased to 0.25 ($n = 19$) with November latitude. The 4 month persistence suggests preservation of memory on a seasonal time scale.

3.2. Relationship Between Land-Fast Sea Ice Breakup and Climatological Forcing

To investigate the reasons behind the interannual and long-term variations of April breakup latitude, the breakup latitude was compared with monthly atmospheric observations (Figure 3b). Significant correlation was found with sea surface pressure in April (−0.68, $n = 20$) and in March (−0.53), suggesting that low pressure coincides with southward breakup. Correlation was 0.44 with mean wind speed in March and 0.42 with

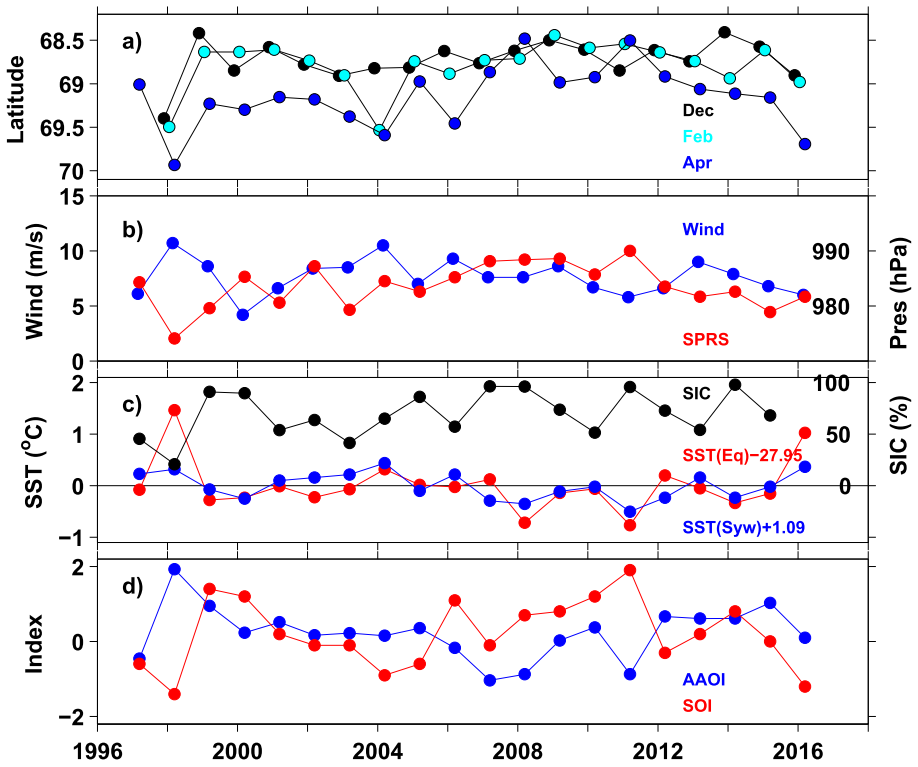

Figure 3. Time series showing the annual latitude of the land-fast ice sea edge in Lützow-Holm Bay compared to environmental parameters and indices. (a) Ice-edge latitudes in April, February, and December; (b) monthly mean sea surface pressure in April and wind speed in March; (c) sea surface temperature near Syowa Station (blue) and in the tropical Pacific (red) and sea ice concentration near Syowa Station (black); and (d) values for the Southern Oscillation Index (SOI) and Southern Hemisphere Annular Mode index (AAOI) in April.

air temperature in March. The number of days with southerly maximum wind in March was negatively correlated (−0.45) with April breakup latitude, which does not support the idea of direct wind-drift breakup.

Oceanic variables revealed higher agreement (Figure 3c). Correlation with SST in April at the nearest point was 0.80 and was over 0.6 from the preceding December. Correlation in April was robust since attempts such as detrend or elimination of large signals before 1998 and of 2016 did not much change the coefficient. Correlation between the nearest-point SST and Syowa Station surface pressure in April was −0.52, suggesting a local link between ocean and atmosphere. The high correlation was also consistent with the high agreement between the breakup latitude and SIC at the nearest pack-ice region (−0.63; negative indicates southward breakup with less SIC). Hence, the change in oceanic heat storage might have affected the local wind response and surface ice cover, changing the wind speed and swells and hence swell propagation [e.g., *Higashi et al.*, 1982], although there is no further quantitative evidence on the detailed mechanism.

The area of high correlation between breakup latitude and SST in April extends broadly along the coast for 0°–60°E, corresponding to the eastern end of the Weddell Gyre (Figure 4a). However, the accuracy and representativeness of SST along the Antarctic coast are likely influenced by the presence of sea and land ice. In addition to the locally high correlation, our correlation map exhibited the highest values (>0.8) in the tropical Pacific around 120°–140°W, slightly south of the equator. The correlation was again robust because detrend did not change the correlation coefficient, although elimination of the large signals above slightly reduced the coefficient to 0.62. This significant correlation was also obtained from the ERSSTv4 (0.73) and HadSST3 (0.68) data sets. From there, the alternating negative and positive correlations propagated to the region off Queen Maud Land. The overall propagating pattern was basically the same for time lags at least until December (Figure 4b). This pattern is similar to that of the Pacific-South American Mode-1 [*Mo and Peagle*, 2001], strongly suggesting teleconnection from the tropical Pacific to the Indian Ocean off Antarctica.

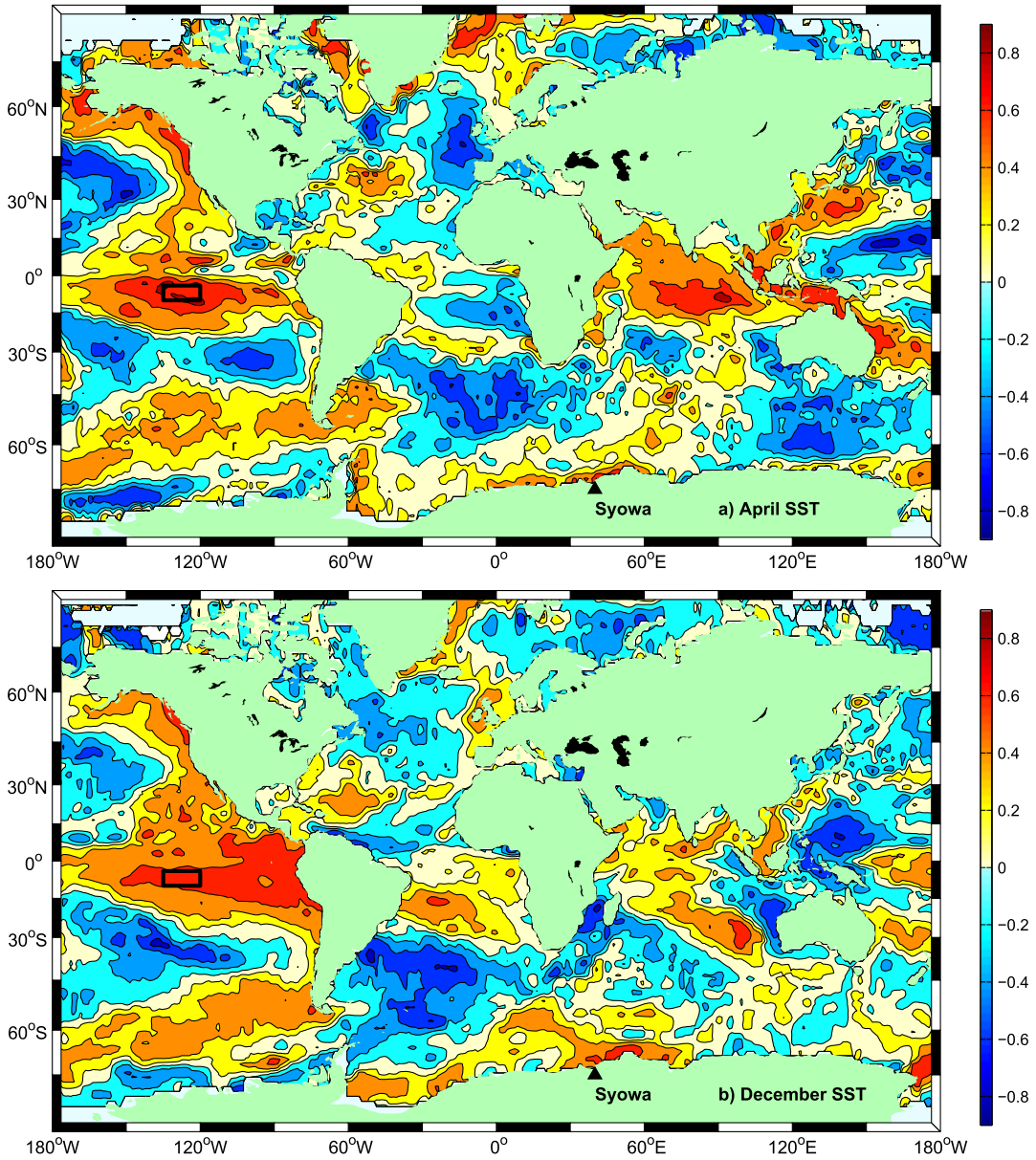

Figure 4. Map showing correlation values between the latitude of the land-fast sea ice edge in Lützow-Holm Bay and SST (a) in April and (b) in December. Syowa Station is located along this bay. The area (120°–135°W, 4°–10°S) used for regression is enclosed by a solid line.

Given the statistical dominance of the tropical teleconnection, the contributions of climate modes to the breakup latitude were examined with the indices. ENSO-related indices revealed persistent correlation with April breakup latitude. Correlation with SOI was −0.55 in April and was even larger (up to −0.64) for the preceding several months and was still significant (−0.62) in the preceding May. Correlations with NINO3 and NINO3.4 were 0.49 and 0.52 in April, respectively, and were 0.70 and 0.68 in the preceding October. Results of previous studies are consistent with the ENSO teleconnection and its local response. In summer, off Queen Maud Land, negative anomalies in sea surface pressure and positive anomalies in SST have been found for El Niño events, as interpreted from *Welhouse et al.* [2016]. Short-wave heat flux might cause the SST anomaly in this region [*Ciasto and England*, 2011]. Hence, together with the previous studies, a possible scenario is as follows: in warm episodes (El Niño), high tropical SST in summer changes the atmospheric circulation off Queen Maud Land through the standing Rossby wave

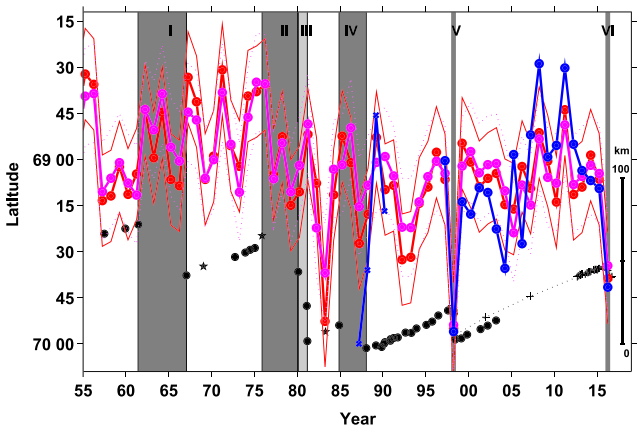

Figure 5. Time series showing the latitude of observed (blue dots and crosses) and reconstructed land-fast sea ice edges in Lützow-Holm Bay. The dots are same as in Figure 3a, while the crosses are obtained from the AVHRR images from *Yamanouchi and Seko* [1992]. Reconstructions were done with ERSSTv4 (red) and HadSST3 (magenta), shown with the standard deviations of the difference from the observation during 1997–2016 (thin solid and dotted lines, respectively). The figure also shows the northernmost latitude of the Shirase Glacier Tongue, taken from *Ushio et al.* [2006] (black dots), aerial photographs (black stars), and MODIS and other satellite images (black crosses). The periods shaded in gray denote intervals that calving-front retreats were observed.

propagation. Associated increase in incoming short-wave radiation off the Antarctic coast can lead to excess heat storage at the ocean surface. Resultant higher SST and less pack-ice cover remain until autumn, and the less ice cover, together with stronger wind, is prone to increase in swell propagation over the land-fast ice. Once the land-fast ice breaks, the ice floes are likely to be carried away by westward coastal current, which is strongest in autumn [*Ohshima et al.*, 1996].

Correlation with SAM was also significant. Correlation was 0.61 with AAO in April. However, lag correlation rapidly dropped to 0.28 in March, revealing no significance for further preceding months. The significant correlation with April AAO might be related to the reinforcement of the pattern for the particular phase combination between ENSO and SAM [*Fogt et al.*, 2011], but the stronger and more persistent correlation with ENSO indices indicates a robust connection with the tropical ocean.

3.3. Land-Fast Sea Ice Breakup and Glacier-Tongue Calving

The calving front of the SGT advanced from the 1950s to 1970s and retreated in the 1980s to 1990s [*Ushio et al.*, 2006]. The position of the SGT calving front is determined by a combination of the timing and magnitude of land-fast sea ice breakup and the advance speed of the glacier tongue. A detailed analysis of breakup timing can help explain what influences the multidecadal variability of the SGT calving front.

The timing of the SGT calving was known with a temporal resolution of a week or two for the event in 1998 (defined as period V) and in 2016 (period VI), and the calving latitude was well-defined (Figure 5). Before that, however, timings of calving were known only with a window of 3 to 5 years, due to a lack of systematic observations. Extrapolation from the timings of irregular observations of changes in calving latitude suggests that calving took place during December (though not specified) 1961 to January 1967 (period I), November 1975 to March 1980 (period II), March 1980 to February 1981 (period III), and December 1984 to January 1988 (period IV).

Does the high correlation with tropical SST explain the breakup and calving timings? Based on the ERSSTv4 and HadSST3 data sets, the SST in April, averaged over 120°–135°W, 4°–10°S, was first regressed to observed April breakup latitude during the 1997–2016 period, and then the regression was extended back in time. Assuming that the April breakup causes calving, the year 1965 and/or 1966 corresponded to period I and 1979 to period II, although the quantitative agreements were not perfect and the retreat in 1980–1981 did not clearly correspond, revealing the complicated nature of land-fast sea ice behavior. The year 1987 corresponded to period IV, and an AVHRR image from April 1987 revealed a large ice breakup [*Yamanouchi and Seko*, 1992]. Moreover, the reconstructed breakup latitude during 1987–1990 matched nicely with the satellite record (Figure 5). Hence, the years of five out of six observed calving events can correspond to those of warm episodes of equatorial SST.

The tropical SST had an ENSO-like multidecadal pattern with a warmer shift after 1976–1977 [*Zhang et al.*, 1997]. The SST-reconstructed breakup latitude revealed strong and frequent poleward shifts during the late 1970s through early 1990s. Hence, the multidecadal variation of the calving front is likely controlled

by the multidecadal variability of breakup latitude driven by the tropical SST, which reinforces the effects of tropical teleconnection.

4. Concluding Remarks

Numerous studies show that the El Niño/Southern Oscillation affects the Antarctic atmosphere, ocean, and sea ice [e.g., *Turner*, 2004]. Around the Antarctic Peninsula, "upstream" of Lützow-Holm Bay on the way from the tropical Pacific, other studies report dipole structure of atmosphere/ocean/sea ice anomalies [*Yuan and Martinson*, 2001] and changes in upper ocean heat storage and stratification [*Meredith et al.*, 2004; *Martinson and Iannuzzi*, 2003] in association with ENSO. In order to connect the large-scale settings with local forcings such as ocean swell and ice structure in Lützow-Holm Bay, and to fully explain the intensity of breakup events, ground-truth evidence from in situ ocean and sea ice observations are required.

Given the widespread nature of this teleconnection, the impacts of glacial freshwater flux on land-fast sea ice variability are not necessarily confined to Lützow-Holm Bay. From January to April 2016, four giant icebergs (D23 to D26) appeared in the record of National Ice Center for 0–90°E, which is unusual. Along the Pacific coast of Antarctica, multidecadal variability has been detected for the calving fronts of outlet glaciers [*Miles et al.*, 2013], and the variability is attributed to phase changes within SAM. The role of widespread oceanic impacts and global climate modes could be indispensable for resolving interactions and long-term variability between local oceans, sea ice, and land ice.

Acknowledgments

The author thanks Shuki Ushio for his invaluable comments and efforts in compiling existing data. The author thanks the National Institute of Polar Research for providing NOAA AVHRR images (http://polaris.nipr.ac.jp/~noaa/noaa_view.html). The atmospheric observations were provided by Japan Meteorological Agency (http://www.data.jma.go.jp/obd/stats/etrn), and aerial photography are obtained by the Geospatial Information Authority of Japan (http://antarctic.gsi.go.jp/index.html). OISSTv2 and ERSSTv4 were obtained from NOAA (http://www.esrl.noaa.gov/psd/data/gridded/data.noaa.oisst.v2.html and https://www1.ncdc.noaa.gov/pub/data/cmb/ersst/v4/netcdf/). Aqua MODIS images were available from NASA (https://worldview.earthdata.nasa.gov/). HadSST3 were obtained from Hadley Center (http://www.metoffice.gov.uk/hadobs/hadsst3/data/download.html). ENSO and AAO indices were provided by NOAA (https://www.ncdc.noaa.gov/teleconnections/enso/indicators/soi/, http://www.cpc.ncep.noaa.gov/data/indices/, and http://www.cpc.ncep.noaa.gov/products/precip/CWlink/daily_ao_index/aao/aao_index.html). Sea ice concentration was obtained at http://nsidc.org/data/docs/daac/nsidc0079_bootstrap_seaice.gd.html. This work was supported by the Grant-in-Aid for Scientific Research (25281001) of the MEXT of the Japanese government.

References

Bajish, C. C., S. Aoki, B. Taguchi, N. Komori, and S.-J. Kim (2013), Quasi-decadal circumpolar variability of Antarctic sea ice, *SOLA*, *9*, 32–35, doi:10.2151/sola.2013-008.

Ciasto, L. M., and M. H. England (2011), Observed ENSO teleconnections to Southern Ocean SST anomalies diagnosed from a surface mixed layer heat budget, *Geophys. Res. Lett.*, *38*, L09701, doi:10.1029/2011GL046895.

Enomoto, H., F. Nishio, H. Warashina, and S. Ushio (2002), Satellite observation of melting and break-up of fast ice in Lützow-Hom Bay, East Antarctica, *Polar Meteorol. Glaciol.*, *16*, 1–14.

Fedotov, V. I., N. V. Cherepanov, and K. P. Tyshko (1998), Some features of the growth, structure and metamorphism of East Antarctic landfast sea ice, in *Antarctic Sea Ice: Physical Processes, Interactions and Variability, Antarct. Res. Ser.*, vol. 74, edited by M. O. Jeffries, pp. 343–354, AGU, Washington, D. C.

Fogt, R. L., D. H. Bromwich, and K. M. Hines (2011), Understanding the SAM influence on the South Pacific ENSO teleconnection, *Clim. Dyn.*, *36*, 1555–1576.

Fraser, A. D. (2011), East Antarctic landfast sea ice distribution and variability, PhD thesis, Univ. of Tasmania.

Fraser, A. D., R. A. Massom, K. J. Michael, B. K. Galton-Fenzi, and J. L. Lieser (2012), East Antarctic landfast sea ice distribution and variability, 2000–08, *J. Clim.*, *25*, 1137–1156, doi:10.1175/JCLI-D-10-05032.1.

Higashi, A., D. J. Goodman, S. Kawaguchi, and S. Mae (1982), On the cause of the break-up of the fast-ice near Syowa Station, East Antarctica on March 18, 1980, *Mem. Natl Inst. Polar Res., Spec. Issue*, *24*, 222–231.

Martinson, D., and R. A. Iannuzzi (2003), Spatial/temporal patterns in Weddell gyre characteristics and their relationship to global climate, *J. Geophys. Res.*, *108*(C4), 8083, doi:10.1029/2000JC000538.

Massom, R. A., K. Hill, C. Barbraud, N. Adams, A. Ancel, L. Emmerson, and M. Pook (2009), Fast ice distribution in Adélie Land, East Antarctica: Interannual variability and implications for Emperor penguins (*Aptenodytes forsteri*), *Mar. Ecol. Prog. Ser.*, *374*, 243–257.

Meredith, M. P., I. A. Renfrew, A. Clarke, J. C. King, and M. A. Brandon (2004), Impact of the 1997/98 ENSO on the upper waters of Marguerite Bay, Western Antarctic Peninsula, *J. Geophys. Res.*, *109*, C09013, doi:10.1029/2003JC001784.

Miles, B. W. J., C. R. Stokes, A. Vieli, and N. J. Cox (2013), Rapid, climate-driven changes in outlet glaciers on the Pacific coast of East Antarctica, *Nature*, *500*, 563–566, doi:10.1038/nature12382.

Miles, B. W. J., C. R. Stokes, and S. S. R. Jamieson (2016), Simultaneous disintegration of outlet glaciers in Porpoise Bay (Wilkes Land), East Antarctica, and the long-term speed-up of Holmes Glacier, *Cryosphere Discuss.*, doi:10.5194/tc-2016-151.

Mo, K. C., and J. N. Peagle (2001), The Pacific-South American Modes and their downstream effects, *Int. J. Climatol.*, *21*, 1211–1229, doi:10.1002/joc.685.

Moriwaki, K., and Y. Yoshida (1990), *Bathymetric Chart of Lützow-Holmbukta, Antarctica, 1: 250 000*, *Special Map Series 4*, Natl Institute of Polar Res, Tokyo.

Nakamura, K., T. Yamannokuchi, K. Doi, and K. Shibuya (2016), Net mass balance calculations for the Shirase Drainage Basin, East Antarctica, using the mass budget method, *Polar Sci.*, *10*(111–122).

Nakawo, M., Y. Ageta, and A. Yoshimura (1978), Discharge of ice across the Syowa coast, *Mem. Natl. Inst. Polar Res., Spec. Issue*, *7*, 235–244.

Ohshima, K. I., T. Takizawa, S. Ushio, and T. Kawamura (1996), Seasonal variations of the Antarctic coastal ocean in the vicinity of Lützow-Holm Bay, *J. Geophys. Res.*, *101*, 20,617–20,628, doi:10.1029/96JC01752.

Thiebaux, H. J., and F. W. Zwiers (1984), The interpretation and estimation of effective sample size, *J. Climate Appl. Meteorol.*, *23*, 800–811.

Trenberth, K. E. (1984), Some effects of finite sample size and persistence on meteorological statistics. Part I: Autocorrelations, *Mon. Weather Rev.*, *112*, 2359–2368.

Turner, J. (2004), Review the El Niño–Southern Oscillation and Antarctica, *Int. J. Climatol.*, *24*, 1–31, doi:10.1002/joc.965.

Ushio, S. (2006), Factors affecting fast-ice break-up frequency in Lützow-Holm Bay, Antarctica, *Ann. Glaciol.*, *44*, 177–182.

Ushio, S., H. Wakabayashi, and F. Nishio (2006), Sea ice variation in Lützow-Holmbukta, Antarctica, during the last fifty years, *Seppyo*, *68*, 299–305.

Welhouse, L. J., M. A. Lazzara, L. M. Keller, G. J. Tripoli, and M. H. Hitchman (2016), Composite analysis of the effects of ENSO events on Antarctica, *J. Clim.*, *29*, 1797–1808.
Yamanouchi, T., and K. Seko (1992), *Antarctica from NOAA Satellites, -Clouds, Ice and Snow-*, 91 pp., Natl. Inst. Polar Res., Tokyo.
Yuan, X., and D. G. Martinson (2001), The Antarctic dipole and its predictability, *Geophys. Res. Lett.*, *28*, 3609–3612, doi:10.1029/2001GL012969.
Zhang, Y., J. M. Wallace, and D. S. Battisti (1997), ENSO-like interdecadal variability: 1900–93, *J. Clim.*, *10*, 1004–1020.